T H E U N I V E R S I T Y O F M I C H I G A N

COLLEGE OF ENGINEERING
Department of Engineering Mechanics

Technical Report

AXIALLY SYMMETRIC IDENTATION OF COHESIONLESS SOILS

L. A. Larkin

ORA Project 04403

under contract with:

DEPARTMENT OF THE ARMY
ORDNANCE TANK-AUTOMOTIVE COMMAND
DETROIT ORDNANCE DISTRICT
CONTRACT NO. DA-20-018-ORD-23276
DETROIT, MICHIGAN

administered through

OFFICE OF RESEARCH ADMINISTRATION ANN ARBOR

September 1963

TABLE OF CONTENTS

LIST OF FIGURES

SUMMARY

The stress distribution in a cohesionless soil, with weight, indented by a smooth, rigid punch is discussed. The governing equations are hyperbolic, and computational procedures based on the method of characteristics are developed. Detailed numerical solutions obtained on the IBM 7090 computer at The University of Michigan are presented for angles of friction of 20°, 25°, 30°, 35°, and 40°.

I. INTRODUCTION

This investigation is concerned with the determination of the stress distribution in a granular material when the material is indented by a smooth, flat-ended circular punch. The material is assumed to be cohesionless and to obey the Coulomb yield criterion. Shield[1] has investigated the axially symmetric behavior of an ideally plastic material which obeys the Tresca yield criterion and he has given a detailed discussion of the indentation problem for this material. Shield's analysis has been extended to materials which obey the Coulomb criterion by Cox, Eason, and Hopkins[2] for the case of weightless material and by Cox[3] for the material with weight. The stress fields computed by Cox[3] were for the particular case where the atmospheric pressure acts as a surcharge. This case is not normally met in practice, and in this paper the numerical work is extended to the more usual circumstance of zero surcharge.

II. GOVERNING EQUATIONS

It will be assumed that the material yields under a general state of stress according to the Coulomb criterion. The cross-section, σ_θ = const., of the resulting yield surface plotted in principal stress space (see Shield[4]) is shown in Figure 1. Taking advantage of the symmetry of this yield surface the discussion will be limited to the sides and corners where $\sigma_1 \geq \sigma_2$. Cox, Eason, and Hopkins[2] have investigated the type of axially symmetric solution associated with each side and corner, called regimes. Only the kinematically determinate group, regimes AB and EF, and the statically determinate group, regimes A and F, give non-trivial stress or velocity solutions. The latter group appears to be the more promising for the solution of the indentation problem.

For the corners A and F the circumferential stress σ_θ is equal to one of the principal stresses in the r-z plane and the limiting Coulomb shear stresses act in this plane. Introducing the variables η and σ_o, where η is the inclination from the r-axis of the clockwise rotating limiting shear stress (see Figure 2) and σ_o is the radius of the Mohr's circle for stress, then, from Figure 3, stress components satisfying the Coulomb yield criterion are:

$$\sigma_r = (c \cot\phi - \sigma_o \operatorname{cosec}\phi) - \sigma_o \sin(\phi + 2\eta) \tag{1a}$$

$$\sigma_z = (c \cot\phi - \sigma_o \operatorname{cosec}\phi) + \sigma_o \sin(\phi + 2\eta) \tag{1b}$$

$$\tau_{zr} = (c \cot\phi - \sigma_o \operatorname{cosec}\phi) \cos(\phi + 2\eta) \tag{1c}$$

$$\sigma_\theta = (c \cot\phi - \sigma_o \operatorname{cosec}\phi) + \bar{w}\,\sigma_o \tag{1d}$$

where

ϕ - angle of friction

c - cohesion

$$\bar{w} = \begin{cases} +1 \text{ for regime F} \\ -1 \text{ for regime A} \end{cases}$$

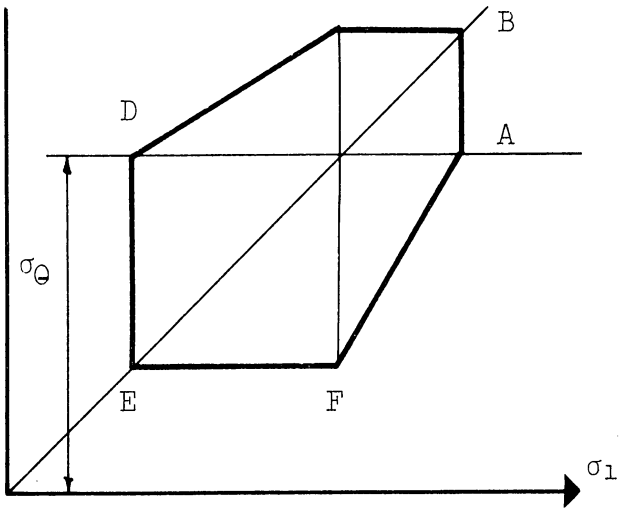

Figure 1. Section of Coulomb yield surface with plane σ_Θ = constant.

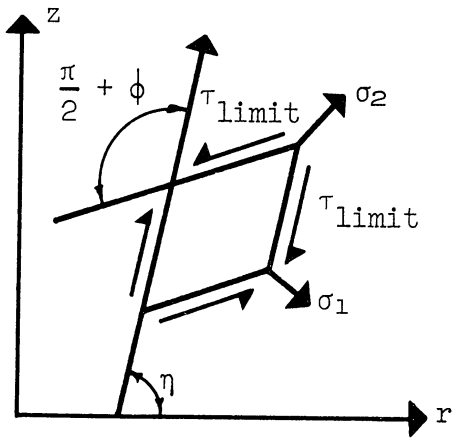

Figure 2. Principal stress directions and limiting shear stress directions.

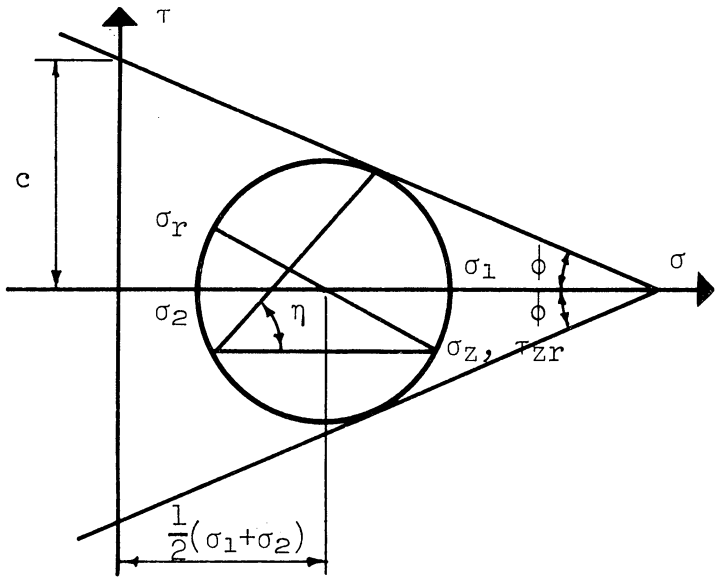

Figure 3. Mohr's circle representation of the limiting stress state.

These equations, together with the equilibrium equations

$$\frac{\partial \sigma_r}{\partial r} + \frac{\partial \tau_{zr}}{\partial z} + \frac{\sigma_r - \sigma_\theta}{r} = 0 \tag{2a}$$

$$\frac{\partial \tau_{zr}}{\partial r} + \frac{\partial \sigma_z}{\partial z} + \frac{\tau_{zr}}{r} + \gamma = 0 \tag{2b}$$

where γ-weight density of the material, form a hyperbolic set of equations. The characteristics are described by

$$\frac{dz}{dr} = \begin{cases} \tan \eta & (3a) \\ \tan \left(\eta + \frac{\pi}{2} + \phi\right) & (3b) \end{cases}$$

The characteristics given by Eq. (3a) will be denoted first characteristics and those described by Eq. (3b) will be called second characteristics. Expressing each length in terms of a fundamental length R and introducing the dimensionless stress $F = \sigma_o/R\gamma$, the variation of F and η along the characteristic directions is given by

$$dF + 2 \tan \phi \, F \, d\eta + F \frac{\tan \phi}{r} \left[\bar{w} \cos \phi \, dr + (1-\bar{w} \sin \phi) \, dz\right] \tag{4a}$$

$$- \tan \phi \, (\sin \phi \, dr + \cos \phi \, dz) = 0$$

on the first characteristics and by

$$dF - 2 \tan \phi \, F \, d\eta + F \frac{\tan \phi}{r} \left[\bar{w} \cos \phi \, dr - (1-\bar{w} \sin \phi) \, dz\right] \tag{4b}$$

$$+ \tan \phi \, (\sin \phi \, dr - \cos \phi \, dz) = 0$$

on the second characteristics.

III. ANALYSIS OF THE PROBLEM

Let the material occupy the region $z \geq 0$ with the origin of coordinates located at the center of the indenter, and set the radius of the indenter as the fundamental length R. Assume that the cylindrical indenter is rigid, flat ended, and perfectly smooth. (The assumption of perfect smoothness is sufficient to render the problem statically determinate.) The stress boundary conditions under the indenter are then

$$\tau_{zr} = 0 \text{ for } 0 \leq r < R ; \quad z = 0 \tag{5}$$

The regimes A and F are distinguished by comparing the relative magnitude of the unequal principal stress with that of the two equal ones. At A the unequal principal stress is larger and at F it is smaller than the two equal stresses. It seems reasonable to suppose that the vertical stress under the indenter is smaller (larger negatively) than the radial or circumferential stresses. At or near the free surface, the radial stress is probably smaller than the vertical stress, which is zero at the surface, and it might well be smaller than the circumferential stress. This suggests the use of regime F throughout and in consequence, $\overline{w} = +1$ will be used in the equations along the characteristics.

The flat surface of the granular material outside the punch surface is usually stress free. (The atmosphere will not provide a confining pressure unless the surface is sealed off and the air evacuated from the material.) The boundary conditions on the free surface are then

$$\tau_{rz} = \sigma_z = 0 \text{ on } r > R ; \quad z = 0 \tag{6}$$

Expressing these boundary conditions in terms of the dependent variables η and F

$$\begin{aligned} \eta &= \frac{\pi}{4} - \frac{\phi}{2} \qquad \text{on } r > R ; \; z = 0 \\ F &= \frac{c}{\gamma R} \operatorname{cotan} \left(\frac{\pi}{4} - \frac{\phi}{2}\right) \end{aligned} \tag{7}$$

For a cohesionless material F vanishes and the direction of the characteristics is undetermined, but if a cohesionless material is considered as the limiting state as the cohesion, c, approaches zero, then it is seen that

$$\eta = \frac{\pi}{4} - \frac{\phi}{2}; \quad F = 0 \quad \text{on } r > R; \quad z = 0 \tag{8}$$

Similarly, expressing Eq. (5), the boundary conditions under the punch, in terms of the variables F and η yields

$$\eta = \frac{3}{4}\pi - \frac{\phi}{2}$$

$$\frac{\sigma_z}{\gamma R} = -\left[F\,(1 + \operatorname{cosec}\phi) - \frac{c}{\gamma R}\operatorname{cotan}\phi\right] \qquad \text{on } 0 \leq r < R; \quad z = 0 \tag{9}$$

From the boundary conditions Eqs. (8) and (9), it can be seen that the characteristics must change their angle rapidly in going from the stress free boundary to the flat indenter boundary. This suggests a field of characteristics as shown in Figure 4 in which a fan of characteristics centered at the edge of the punch accomplishes the required change in angle. Such a type of field is to be expected from the solution of the analogous plane strain problem and from the circular indentation solutions by Cox[2] and Shield.[4] The fan center, point A, is the point of intersection for all of the first characteristics in the fan, hence the inclination of the first characteristics takes on many values here. Just to the right of A the boundary conditions are given by Eq. (8) and so the characteristic at the edge of the fan, AC, is initially inclined at $\pi/4 - \phi/2$ to the r-axis. The conditions just to the left of A are given by Eq. (9) and hence the characteristic, AD, starts out at $3/4\pi - \phi/2$ to the r-axis. This limits the included angle of the fan to $\pi/2$.

The variation of the stress variable, F, around the singular point A can be found by considering the point to be a degenerate second characteristic of zero length. Then Eq. (4b) becomes

$$d\,(\operatorname{cotan}\phi\ \ell n\ F) - 2d\eta = 0$$

Integrating and imposing the known conditions at the free boundary, Eq.(7), the variation of the stress parameter around the singularity becomes

$$\ell n \left[\frac{F}{\frac{c}{R\gamma} \frac{\cos \phi}{1 - \sin \phi}} \right] = 2 \left[\eta - \left(\frac{\pi}{4} - \frac{\phi}{2} \right) \right] \tan \phi . \qquad (10)$$

For the case of a cohesionless material, the logarithmic term becomes indefinitely large and the only way to preserve the equality (10) is to set $F = 0$. Hence all the stress components are zero if the singularity is approached from any direction.

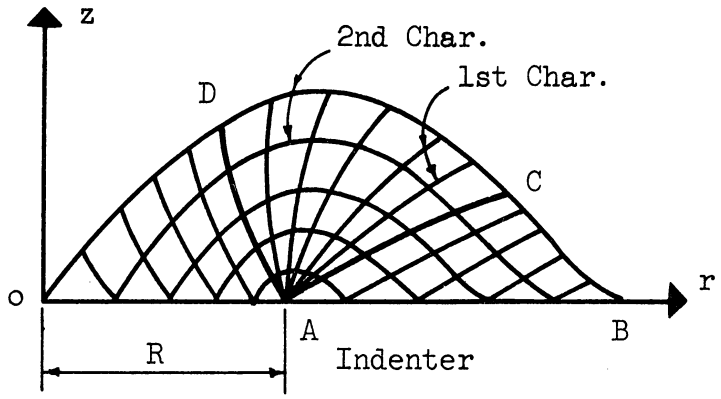

Figure 4. Field of stress characteristics.

IV. SOLUTION OF THE PROBLEM

The field of characteristics and the stress field can be obtained by the integration of the differential equations involving F and η along the characteristics simultaneously with the differential equations of the characteristics themselves. The solution of these equations usually involves a numerical procedure because of the difficulties in obtaining an analytical solution. The numerical procedure is based on the approximation of Eqs. (3) and (4) by finite difference equations. These finite difference equations are in turn used to extend the solution from the boundary values.

In the usual situation, F, η, r, and z are known at two intersections P, Q of the characteristics. It is desired to extend the solution to point 1, (see Figure 5). The unknown coordinates (r_1, z_1) can be initially approximated by finding the intersection of the two characteristics extended at their initial inclination. However, subsequent approximations for r_1 and z_1 can be made more accurately by extending each characteristic one-half its projection at its initial angle and the second half at the approximated angle of that characteristic at the point being determined. Therefore, if half the vertical projection is used then r_1 and z_1 are found by solving

$$\frac{r_1 - r_P}{z_1 - z_P} = \frac{1}{2}(\cot\eta_P + \cot\eta_1) \quad \text{for first characteristic and} \tag{11a}$$

$$\frac{r_1 - r_Q}{z_1 - z_Q} = \frac{1}{2}[\cot(\eta_Q + \pi/2 + \phi) + \cot(\eta_1 + \pi/2 + \phi)] \quad \text{for the} \tag{11b}$$

second characteristic. The equations on the dependent variables F and η along the characteristics, Eqs. (4), will be replaced by the finite difference equations

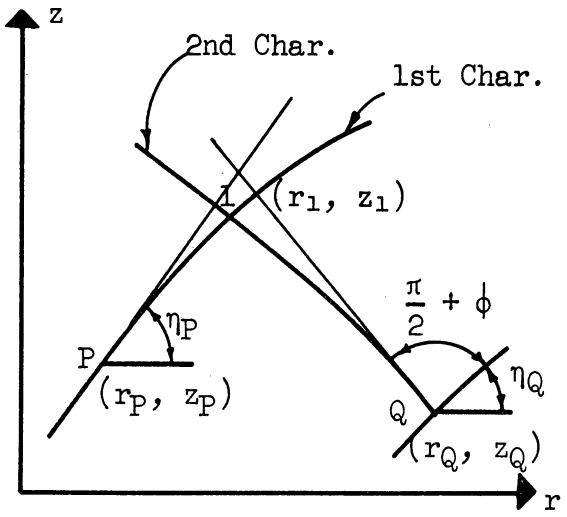

Figure 5. Illustration of typical calculation situation.

$$F_1 - F_P + 2 \tan \phi \left(\frac{F_1 + F_P}{2}\right) (\eta_1 - \eta_P) + \left(\frac{F_1 + F_P}{2}\right) \Big/ \left(\frac{r_1 + r_P}{2}\right) \tan \phi$$

$$[\cos \phi \, (r_1 - r_P) + (1 - \sin \phi) \, (z_1 - z_P)] \qquad (12a)$$

$$\tan \phi \, [\sin \phi \, (r_1 - r_P) + \cos \phi \, (z_1 - z_P)] = 0 \quad \text{on a first characteristic.}$$

$$F_1 - F_Q - 2 \tan \phi \left(\frac{F_1 + F_Q}{2}\right) (\eta_1 - \eta_Q) + \left(\frac{F_1 + F_Q}{2}\right) \Big/ \left(\frac{r_1 + r_Q}{2}\right) \tan \phi$$

$$[\cos \phi \, (r_1 - r_Q) - (1 - \sin \phi) \, (z_1 - z_Q)] \qquad (12b)$$

$$\tan \phi \, [\sin \phi \, (r_1 - r_Q) - \cos \phi \, (z_1 - z_Q)] = 0 \quad \text{on a second characteristic.}$$

Solving for F_1 and η_1

$$F_1 = \frac{1}{D}\Bigg[F_P + F_Q - \tan\phi\,[F_P(\eta_1 - \eta_P) - F_Q(\eta_1 - \eta_Q) + \cos\phi$$

$$\left(F_P\left(\frac{r_1 - r_P}{r_1 + r_P}\right) + F_Q\left(\frac{r_1 - r_Q}{r_1 + r_Q}\right)\right) + (1 - \sin\phi)\left(F_P\left(\frac{z_1 - z_P}{r_1 + r_P}\right) - F_Q\left(\frac{z_1 - z_Q}{r_1 + r_Q}\right)\right) \quad (13a)$$

$$- \sin\phi\,(r_Q - r_P) - \cos\phi\,(2z_1 - z_P - z_Q)]\Bigg]$$

where

$$D = 2 + \tan\phi\left[\eta_Q - \eta_P + \cos\phi\left(\frac{r_1 - r_P}{r_1 + r_P} + \frac{r_1 - r_Q}{r_1 + r_Q}\right)\right.$$

$$\left. + (1 - \sin\phi)\left(\frac{z_1 - z_P}{r_1 + r_P} - \frac{z_1 - z_Q}{r_1 + r_Q}\right)\right]$$

$$\eta_1 = \frac{1}{2}\Bigg[\eta_P + \eta_Q - \cos\phi\left(\frac{r_1 - r_P}{r_1 + r_P} - \frac{r_1 - r_Q}{r_1 + r_Q}\right) - (1 - \sin\phi)\left(\frac{z_1 - z_P}{r_1 + r_P} + \frac{z_1 - z_Q}{r_1 + r_Q}\right)$$

$$+ \cos\phi\left(\frac{z_1 - z_P}{F_1 + F_P} - \frac{z_1 - z_Q}{F_1 + F_Q}\right) + \sin\phi\left(\frac{r_1 - r_P}{F_1 + F_P} + \frac{r_1 - r_Q}{F_1 + F_Q}\right) \quad (13b)$$

$$- \operatorname{cotan}\phi\left(\frac{F_1 - F_P}{F_1 + F_P} - \frac{F_1 - F_Q}{F_1 + F_Q}\right)\Bigg]$$

After the initial approximations for r_1 and z_1 are calculated, η_1 is estimated and a new F_1 and η_1 are calculated from Eqs. (13). Subsequently a new r_1 and z_1 can be found from Eqs. (11) and the iteration performed until successive values become sufficiently unchanged.

In this manner the characteristics and stresses in the region ABC are uniquely determined from the known boundary AB and the boundary values of F and η along it. Following the same procedure the stresses and char-

acteristics are uniquely determined in the fan CAD from the calculated values of F and η along the characteristic AC and from their boundary values at the singularity A. Finally the region ADO is uniquely calculated starting from the previously determined values of the independent variables on the characteristic AD and knowing that the second characteristics terminate on the line $z = 0$ at an inclination of $\pi/4 + \phi/2$ to the r-axis (see Eq. (9)). The radius at which this occurs can be found from Eq. (11b) and the corresponding value of F under the indenter can be found from Eq. (12b) and subsequently substituted into Eq. (9) to find the normal pressure under the indenter.

The above procedure was programmed on the IBM 7090 digital computer at The University of Michigan. The iteration for each point was terminated when the change in every variable (r, z, F and η) fell below 10^{-5} of its previous value. The number of iterations required to attain this accuracy was usually five and it was never more than nine. Whenever a characteristic experienced a change in angle of more than 6° from point to point, the mesh size was decreased locally until this requirement was satisfied. As a result, the mesh size became very small near the singularity point. The largest field calculated required just under six minutes total computer time; each of the others needed less than three minutes total.

The equations in the fan region ACD and consequently in the region ADO were poorly conditioned. Furthermore, it was found that the solution could be improved by the use of a small surface pressure along AB coupled with a very fine mesh at the singularity. This is not an unreasonable step, because in the physical problem the boundary conditions given by Eq. (8) will be perturbed by the initial pre-flow sinkage of the indenter and the slight overburden then added along AB will provide a source for the pressure necessary to make the solution well behaved. A pressure of the order of 10^{-2} Rγ was assumed which corresponds to an initial sinkage of the order of 10^{-2} R where the thin overburden has no strength. The resulting fields of characteristics and pressure distributions under the punch for angles of friction varying from 20°-40° are shown in Figures 6-10 . Figure 11 is a graph of the ratio OB/OA and Figure 12 is a plot of the average indenter pressure. The appendix contains the computer program as written in the Michigan Algorithm Decoder (MAD) language.

An overall equilibrium check equating the resisting forces acting on the outer second characteristic to the combined forces from the soil weight and from the indenter was made for the $\phi = 30°$ case. The error in vertical equilibrium amounted to less than 0.4% of the punch load.

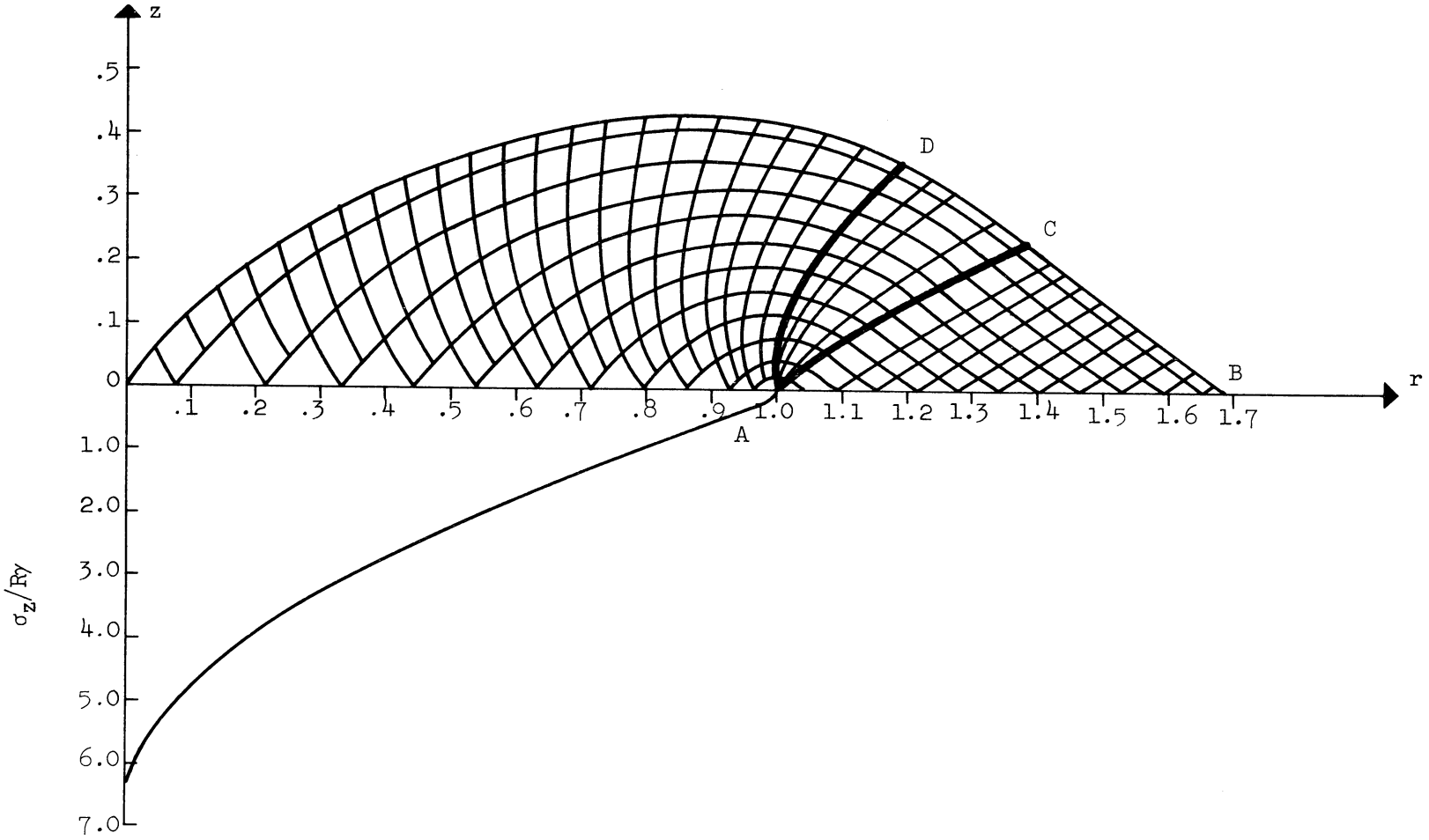

Figure 6. Stress characteristics and punch pressure distribution for $\phi = 20°$.

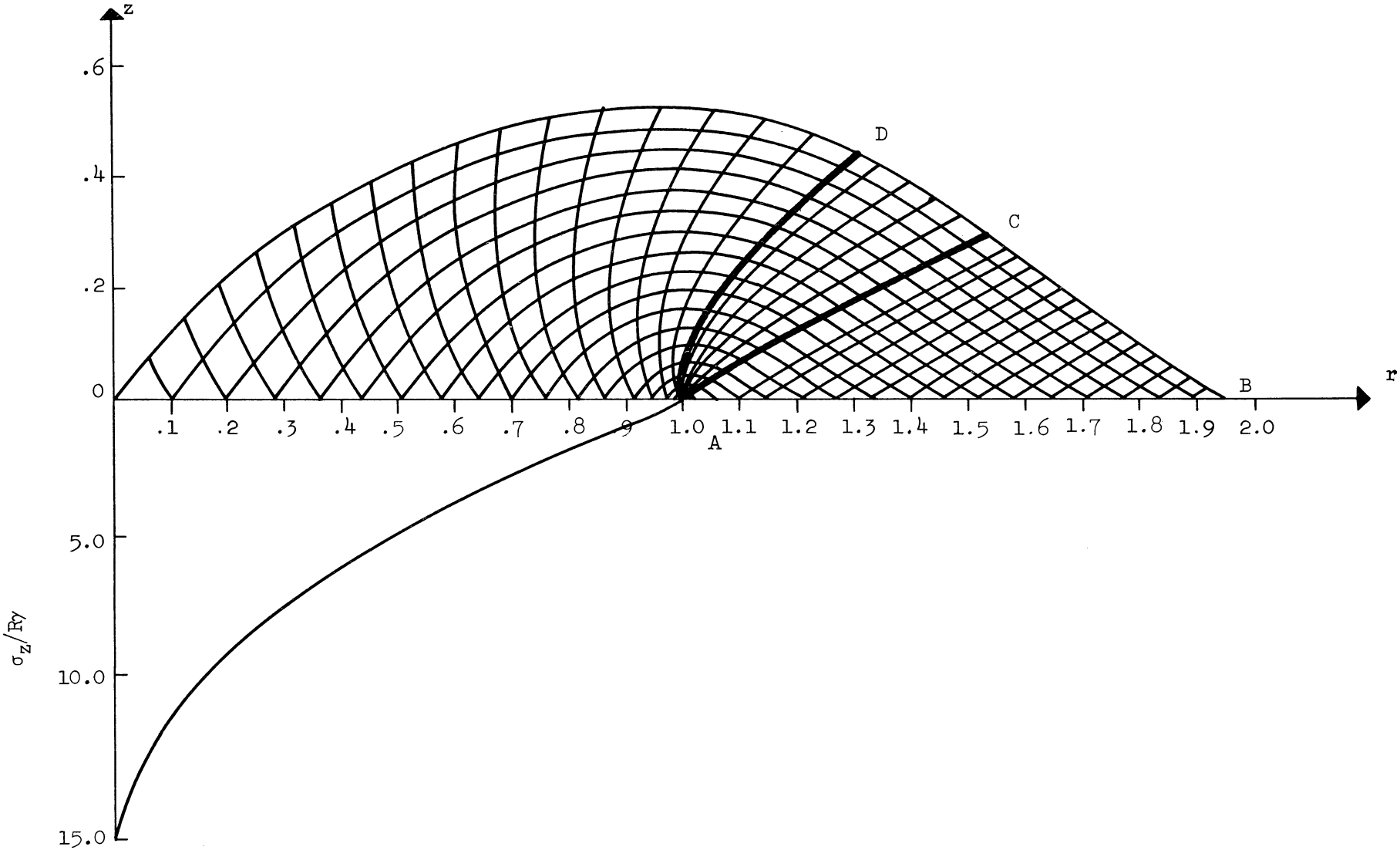

Figure 7. Stress characteristics and punch pressure distribution for $\phi = 25°$.

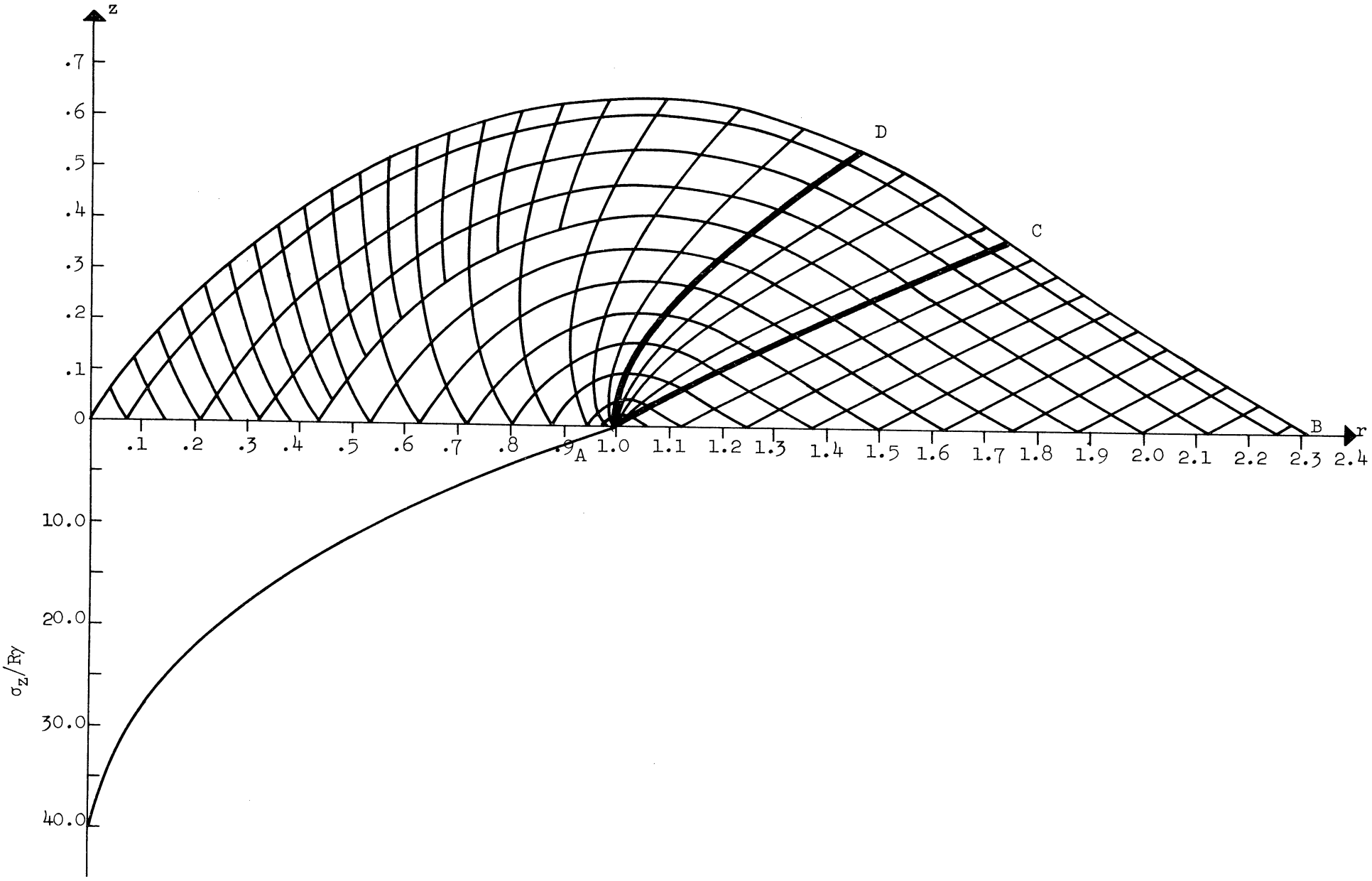

Figure 8. Stress characteristics and punch pressure distribution for $\phi = 30°$.

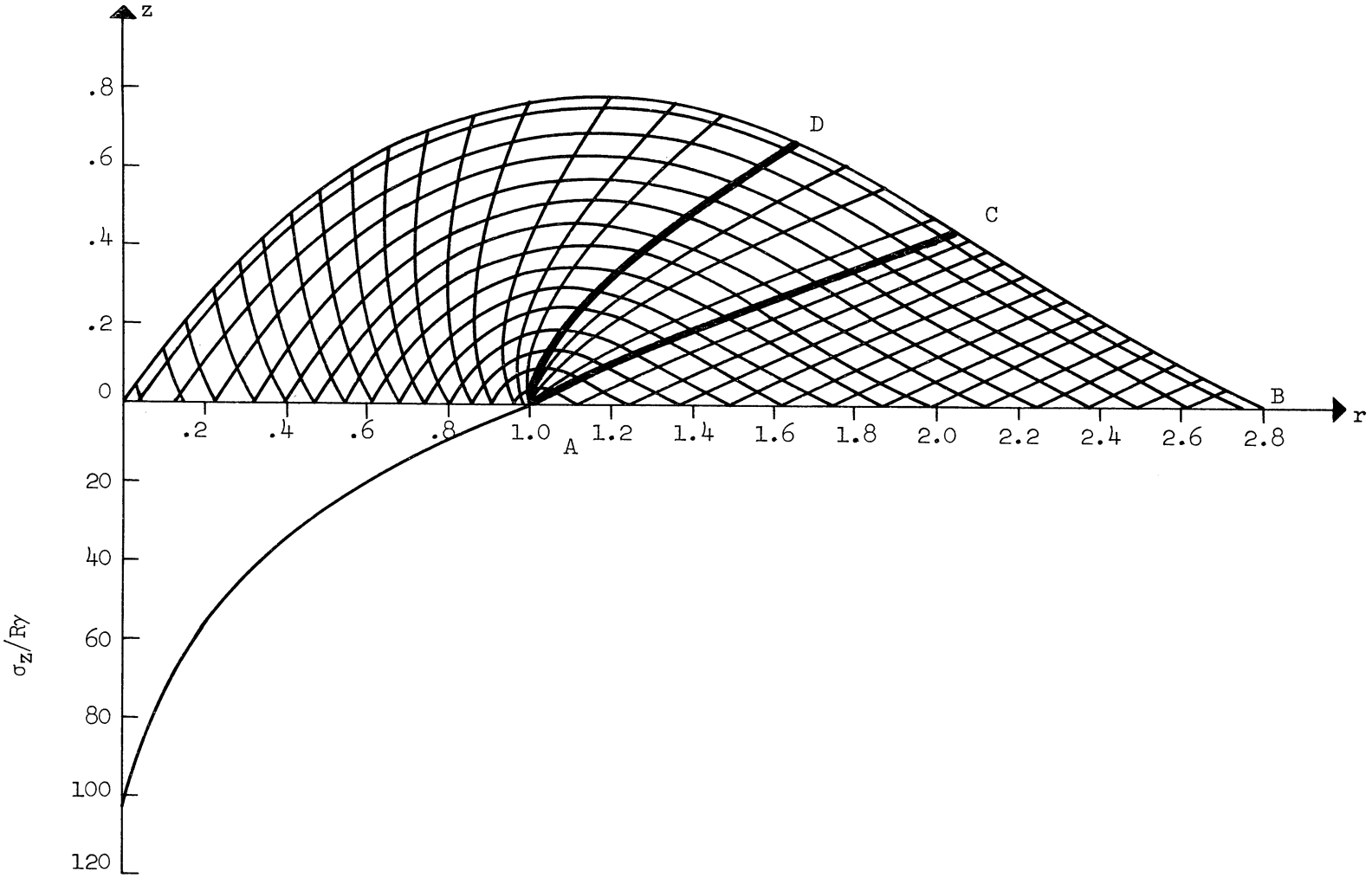

Figure 9. Stress characteristics and punch pressure distribution for $\phi = 35°$.

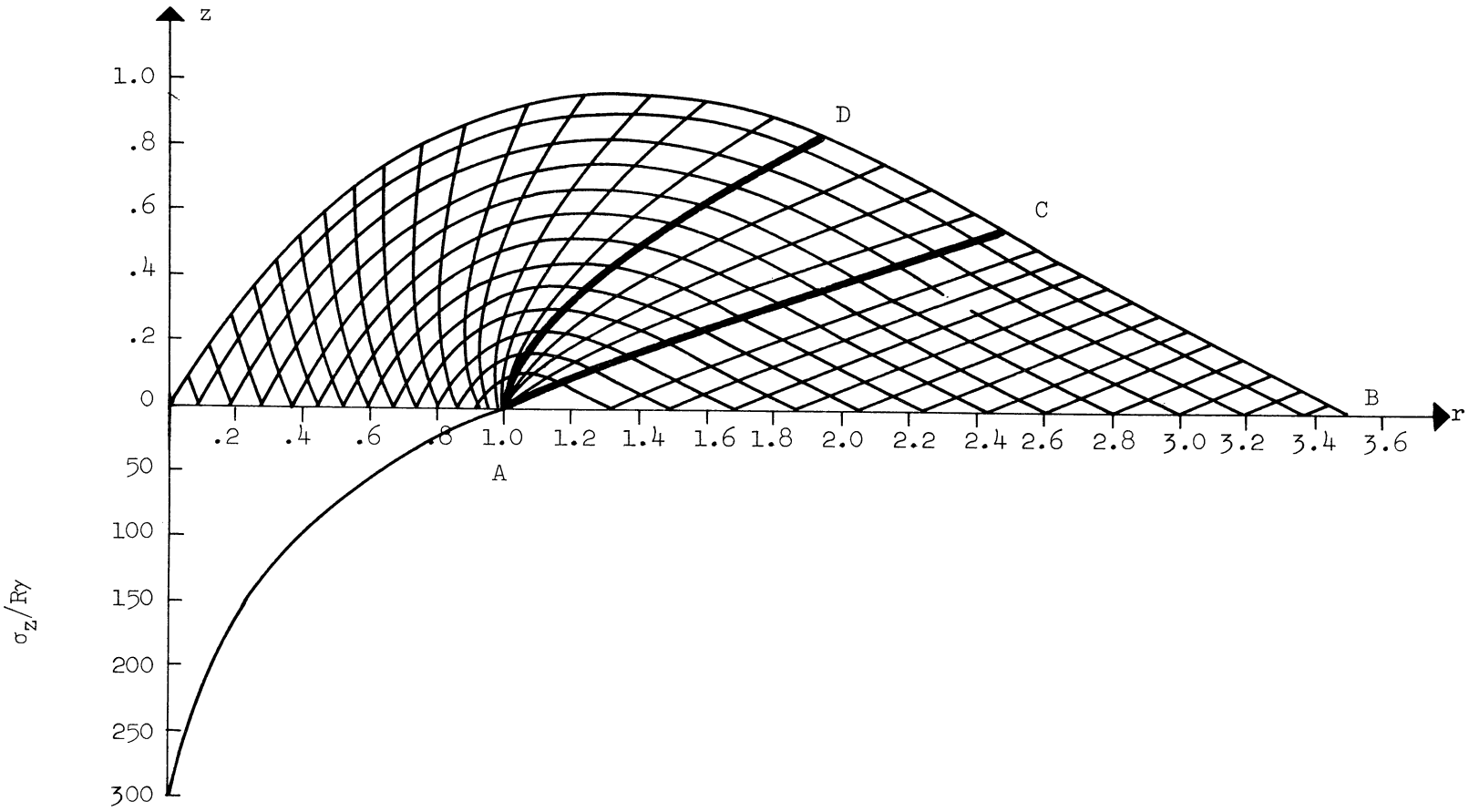

Figure 10. Stress characteristics and punch pressure distribution for $\phi = 40°$.

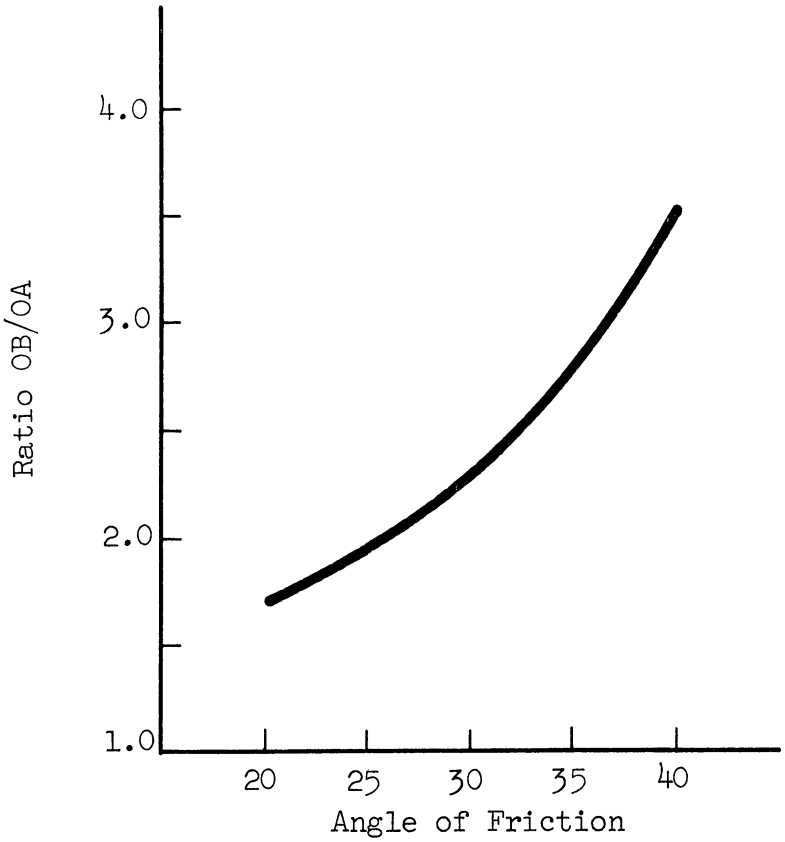

Figure 11. Variation of OB/OA with angle of friction.

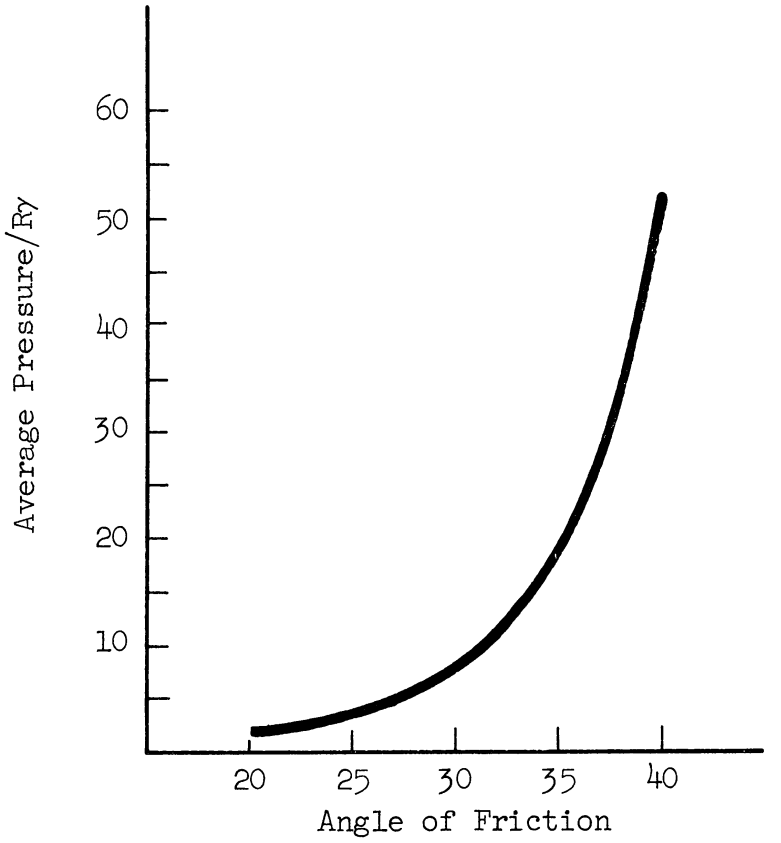

Figure 12. Variation of average punch pressure with angle of friction.

REFERENCES

1. R. T. Shield, "On the Plastic Flow of Metals Under Conditions of Axial Symmetry," Proc. Royal Soc. A, vol. 233, 1955, pp. 267-286.

2. A. D. Cox, G. Eason, and H. G. Hopkins, "Axially Symmetric Plastic Deformation in Soils," Phil. Trans. Royal Soc., vol. 254, A. 1036, 1961, pp. 1-45.

3. A. D. Cox, "Axially Symmetric Plastic Deformation in Soils--II. Indentation of Ponderable Soils," International Journ. of Mech. Sci., vol. 4, 1962, pp. 371-380.

4. R. T. Shield, "On Coulomb's Law of Failure in Soils," Journ. Mech. and Phys. of Solids, vol. 4, 1955, pp. 10-16.

APPENDIX: MAD COMPUTER PROGRAM

```
$COMPILE MAD,EXECUTE,DUMP, PRINT OBJECT
        R
        R    AXIALLY SYMMETRIC PUNCH PROBLEM
        R
START   READ FORMAT INPUT,ANGLE, W, MESH, N, QUIT, P, ALPHA
        PRINT FORMAT HEAD
        PRINT FORMAT OUTPUT,ANGLE, W, MESH, N, QUIT, P, ALPHA
        READ AND PRINT DATA
        PRINT FORMAT TOP
        INTEGER N, M, P, I, J, QUIT, W,QUITO1, QUITO2
        DIMENSION R(5000,MTRX), Z(5000,MTRX), ETA(5000,MTRX),
       1 F(5000,MTRX)
        VECTOR VALUES MTRX=A.,2,0,45
        INTERNAL FUNCTION A.(Q,I,J)=(W+J-1)*(J-1)+I-N+J
        PI=3.1415927
        NUMB=0.
        LAST=0.
        PHI=PI/180.*ANGLE
        SINPHI=SIN.(PHI)
        COSPHI=COS.(PHI)
        TANPHI=SINPHI/COSPHI
        J=1
        M=0
        ETA(N,J)=.25*PI-.5*PHI
        R(N,J)=1.0
        Z(N,J)=0.
        F(N,J)=ALPHA
        PRINT FORMAT RESULT,M,N,J,R(N,J),Z(N,J),180./PI*ETA(N,J),
       1F(N,J)
        THROUGH SAM, FOR I=N+1,1,I.E.N+W+1
        ETA(I,J)=ETA(I-1,J)+.5*PI/W
        R(I,J)=1.0
        Z(I,J)=0.
        F(I,J)=ALPHA*EXP.(2.*TANPHI*(ETA(I,J)-.25*PI+.5*PHI))
SAM     PRINT FORMAT RESULT,M,I,J,R(I,J),Z(I,J),180./PI*ETA(I,J),F(I,
       1J)
        SUM=0.
LOOP    J=J+1
        WHENEVER J.E.QUITO1, MESH=MESHO1
        WHENEVER J.E.QUITO2, MESH=MESHO2
        WHENEVER J.E.QUIT
        WHENEVER NUMB .E.0.
        QUITO1=99
        QUITO2=99
        MESH=MESHO3
        NUMB=1.
        OTHERWISE
        MESH=MESHO3
        END OF CONDITIONAL
        END OF CONDITIONAL
OVER    I=N-J+1
        ETA(I,J)=.25*PI-.5*PHI
        Z(I,J)=0.
        R(I,J)=R(I+1,J-1)+1./MESH
        F(I,J)= ALPHA
        M=0
        TRANSFER TO TEST
BEGIN   I=I+1
        WHENEVER I.E.N+W+J-1
        WHENEVER LAST.E.2.
        TRANSFER TO START
        END OF CONDITIONAL
        END OF CONDITIONAL
        WHENEVER I.E.N+W+J-1
        OLDETA=.75*PI-.5*PHI
        ETA(I,J)=OLDETA
        WHENEVER .ABS.(ETA(I,J)-ETA(I-1,J)).G.INCRE, TRANSFER TO GAK
        TANQ=COS.(ETA(I-1,J)+.5*PI+PHI)/SIN.(ETA(I-1,J)+.5*PI+PHI)
        TAETPH=COS.(OLDETA+.5*PI+PHI)/SIN.(OLDETA+.5*PI+PHI)
        R(I,J)=R(I-1,J)-.5*Z(I-1,J)*(TANQ+TAETPH)
        Z(I,J)=0.
        H=-F(I-1,J)/(R(I,J)+R(I-1,J))*(SINPHI*(R(I,J)-R(I-1,J))-
       1TANPHI*(1.-SINPHI)*(Z(I,J)-Z(I-1,J)))-TANPHI*SINPHI*(R(I,J)
       2-R(I-1,J))+SINPHI*(Z(I,J)-Z(I-1,J))
        F(I,J)=(F(I-1,J)*(1.+TANPHI*(OLDETA-ETA(I-1,J)))+H)/
       1(1.-TANPHI*(OLDETA-ETA(I-1,J))+SINPHI*(R(I,J)-R(I-1,J))/
       2(R(I,J)+R(I-1,J))-TANPHI*(1.-SINPHI)*(Z(I,J)-Z(I-1,J))/
       3(R(I,J)+R(I-1,J)))
        PRINT FORMAT ANSWER, I,J,R(I,J),Z(I,J),180.*ETA(I,J)/PI,
       1  F(I,J)*(1./SINPHI+1.)
        WHENEVER (R(I-1,J-1)-R(I,J)).G.R(I,J)
        WHENEVER LAST.E.0.
        LAST=LAST+1.
        MESH=2.*MESH
        OTHERWISE
        LAST=LAST+1.
        SUM=SUM+(1.+1./SINPHI)*F(I,J)*R(I,J)*R(I,J)
        PRINT FORMAT PRESSR, SUM
        END OF CONDITIONAL
        OTHERWISE
        SUM=SUM+(1.+1./SINPHI)*(F(I,J)+F(I-1,J-1))*.5*(R(I,J)+R(I-1,
       1J-1))*(R(I-1,J-1)-R(I,J))
        END OF CONDITIONAL
        TRANSFER TO LOOP
        END OF CONDITIONAL
        OLDETA=ETA(I,J-1)
        OLDF=F(I,J-1)
        OLDR=R(I,J-1)
        OLDZ=Z(I,J-1)
        ZP=Z(I,J-1)
        ZQ=Z(I-1,J)
        RP=R(I,J-1)
        RQ=R(I-1,J)
        FP=F(I,J-1)
        FQ=F(I-1,J)
        OLDDEV=1.
        M=0
        WHENEVER .ABS.(.5*PI-PHI-OLDETA) .L. .175
        TANP=SIN.(ETA(I,J-1))/COS.(ETA(I,J-1))
        TANQ=SIN.(ETA(I-1,J)+.5*PI+PHI)/COS.(ETA(I-1,J)+.5*PI+PHI)
        BETA=1.
        OTHERWISE
        TANP=COS.(ETA(I,J-1))/SIN.(ETA(I,J-1))
        TANQ=COS.(ETA(I-1,J)+.5*PI+PHI)/SIN.(ETA(I-1,J)+.5*PI+PHI)
        BETA=0.
        END OF CONDITIONAL
ITERAT  WHENEVER M.E.P
        PRINT FORMAT REMARK
        PRINT RESULTS M, I, J, R(I,J), Z(I,J), ETA(I,J), F(I,J)
        TRANSFER TO START
        OTHERWISE
        M=M+1
        END OF CONDITIONAL
        WHENEVER BETA .E. 1.
        TANETA=SIN.(OLDETA)/COS.(OLDETA)
        TAETPH=SIN.(OLDETA+.5*PI+PHI)/COS.(OLDETA+.5*PI+PHI)
        DENOM=TANP+TANETA-TANQ-TAETPH
        R1=(RP*(TANP+TANETA)-RQ*(TANQ+TAETPH)+2.*(ZQ-ZP))/DENOM
        Z1=(ZQ*(TANP+TANETA)-ZP*(TANQ+TAETPH)+.5*(RP-RQ)*(TANP+TANETA
       1)*(TANQ+TAETPH))/DENOM
        OTHERWISE
        TANETA=COS.(OLDETA)/SIN.(OLDETA)
        TAETPH=COS.(OLDETA+.5*PI+PHI)/SIN.(OLDETA+.5*PI+PHI)
        DENOM=TANP+TANETA-TANQ-TAETPH
        Z1=(ZP*(TANP+TANETA)-ZQ*(TANQ+TAETPH)+2.*(RQ-RP))/DENOM
        R1=(RQ*(TANP+TANETA)-RP*(TANQ+TAETPH)+.5*(ZP-ZQ)*(TANP+TANETA
       1)*(TANQ+TAETPH))/DENOM
        END OF CONDITIONAL
        R(I,J)=R1
        Z(I,J)=Z1
        F(I,J)=(FP+FQ-TANPHI*(FP*(OLDETA-ETA(I,J-1))-FQ*(OLDETA-ETA(I
       1-1,J)))+COSPHI*(FP*(R1-RP)/(R1+RP)+FQ*(R1-RQ)/(R1+RQ))+
       2(1.-SINPHI)*(FP*(Z1-ZP)/(R1+RP)-FQ*(Z1-ZQ)/(R1+RQ))-SINPHI*
       3(RQ-RP)-COSPHI*(2.*Z1-ZP-ZQ))/(2.+TANPHI*(ETA(I-1,J)-ETA(I,
       4J-1)+COSPHI*((R1-RP)/(R1+RP)+(R1-RQ)/(R1+RQ))+(1.-SINPHI)*((Z
       51-ZP)/(R1+RP)-(Z1-ZQ)/(R1+RQ))))
        ETA(I,J)=.5*(ETA(I,J-1)+ETA(I-1,J)-COSPHI*((R1-RP)/(R1+RP)
       1 -(R1-RQ)/(R1+RQ))-(1.-SINPHI)*((Z1-ZP)/(R1+RP)+(Z1-ZQ)/(R1+R
       2Q))+COSPHI*((Z1-ZP)/(F(I,J)+FP)-(Z1-ZQ)/(F(I,J)+FQ))+SINPHI*
       3((R1-RP)/(F(I,J)+FP)+(R1-RQ)/(F(I,J)+FQ))-1./TANPHI*
       4((F(I,J)-FP)/(F(I,J)+FP)-(F(I,J)-FQ)/(F(I,J)+FQ)))
        DEV=ETA(I,J)-OLDETA
        WHENEVER .ABS.(Z(I,J)-OLDZ).G.1.E-5*OLDZ.OR.
       1.ABS.(R(I,J)-OLDR).G.1.E-6*OLDR.OR.
       2.ABS.(F(I,J)-OLDF).G.1.E-5*OLDF.OR.
       3.ABS.(ETA(I,J)-OLDETA).G.1.E-5*OLDETA
        WHENEVER DEV*OLDDEV.G.0.
        OLDZ=Z(I,J)
        OLDR=R(I,J)
        OLDF=F(I,J)
        OLDETA=ETA(I,J)
        OLDDEV=DEV
        TRANSFER TO ITERAT
        OTHERWISE
        OLDZ=.5*(Z(I,J)+OLDZ)
        OLDR=.5*(R(I,J)+OLDR)
        OLDF=.5*(F(I,J)+OLDF)
        OLDETA=.5*(ETA(I,J)+OLDETA)
        OLDDEV=DEV
        TRANSFER TO ITERAT
        END OF CONDITIONAL
        END OF CONDITIONAL
        WHENEVER .ABS.(ETA(I,J)-ETA(I-1,J)).G.INCRE
GAK     MESH=2.*MESH
        QUITO1=QUITO1+2
        QUITO2=QUITO2+2
        WHENEVER NUMB.E.1.
        QUIT=J+2
        OTHERWISE
        QUIT=QUIT+2
        END OF CONDITIONAL
        TRANSFER TO OVER
        END OF CONDITIONAL
TEST    PRINT FORMAT RESULT,M,I,J,R(I,J),Z(I,J),180./PI*ETA(I,J),F(I,
       1J)
        TRANSFER TO BEGIN
        VECTOR VALUES INPUT=$F10.3, I10, F10.3, 3I10, E10.5*$
        VECTOR VALUES HEAD=$//18H ANGLE OF FRICTIONS5,12HFAN DIVISION
       1S10, 4HGRIDS10, 1HNS10, 11HPRINT LIMITS11, 15HITERATION LIMIT
       2S3,8HPRESSURE*$
        VECTOR VALUES OUTPUT=$/S2,F10.3,S10,I10  ,S8,F10.3,S8,I3,S12,
       1I3,S22,I3,S8,E10.2*$
        VECTOR VALUES TOP=$//S6,1HMS4,4HI, JS20,1HRS24,1HZS23,
       13HETAS24,1HF//*$
        VECTOR VALUES RESULT=$S5,I2,S2, 2I3,4E25.5*$
        VECTOR VALUES ANSWER=$S9,2I3,3E25.5,13H PRESSURE IS E12.5*$
        VECTOR VALUES REMARK=$17H POOR CONVERGENCE*$
        VECTOR VALUES PRESSR=$/21H AVERAGE PRESSURE IS E12.5*$
        END OF PROGRAM
$DATA
      30.00        24     256.00        30        15        50     1.E-2
QUITO1=6, QUITO2=10, MESHO1=128., MESHO2=64., MESHO3=16.,INCRE=.105*
```

AD Accession No. UNCLASSIFIED

The University of Michigan, Office of Research Administration, Ann Arbor, Mich. Axially Symmetric Indentation of Cohesionless Soils, by L. A. Larkin. Report No. 04403-10-T, Sept. 1963, 23 p. incl. illus., Project 04403 (Contract No. DA-20-018-ORD-23276)

UNCLASSIFIED

The stress distribution in a cohesionless soil, with weight, indented by a smooth, rigid punch is discussed. The governing equations are hyperbolic, (over)

UNCLASSIFIED

and computational procedures based on the method of characteristics are developed. Detailed numerical solutions obtained on the IBM 7090 computer at The University of Michigan are presented for angles of friction of 20°, 25°, 30°, 35°, and 40°.

UNCLASSIFIED

AD Accession No. UNCLASSIFIED

The University of Michigan, Office of Research Administration, Ann Arbor, Mich. Axially Symmetric Indentation of Cohesionless Soils, by L. A. Larkin. Report No. 04403-10-T, Sept. 1963, 23 p. incl. illus., Project 04403 (Contract No. DA-20-018-ORD-23276)

UNCLASSIFIED

The stress distribution in a cohesionless soil, with weight, indented by a smooth, rigid punch is discussed. The governing equations are hyperbolic, (over)

UNCLASSIFIED

UNCLASSIFIED

and computational procedures based on the method of characteristics are developed. Detailed numerical solutions obtained on the IBM 7090 computer at The University of Michigan are presented for angles of friction of 20°, 25°, 30°, 35°, and 40°.

UNCLASSIFIED

AD Accession No. UNCLASSIFIED

The University of Michigan, Office of Research Administration, Ann Arbor, Mich. Axially Symmetric Indentation of Cohesionless Soils, by L. A. Larkin. Report No. 04403-10-T, Sept. 1963, 23 p. incl. illus., Project 04403 (Contract No. DA-20-018-ORD-23276)

UNCLASSIFIED

The stress distribution in a cohesionless soil, with weight, indented by a smooth, rigid punch is discussed. The governing equations are hyperbolic, (over)

UNCLASSIFIED

and computational procedures based on the method of characteristics are developed. Detailed numerical solutions obtained on the IBM 7090 computer at The University of Michigan are presented for angles of friction of 20°, 25°, 30°, 35°, and 40°.

UNCLASSIFIED

AD Accession No. UNCLASSIFIED

The University of Michigan, Office of Research Administration, Ann Arbor, Mich. Axially Symmetric Indentation of Cohesionless Soils, by L. A. Larkin. Report No. 04403-10-T, Sept. 1963, 23 p. incl. illus., Project 04403 (Contract No. DA-20-018-ORD-23276)

UNCLASSIFIED

The stress distribution in a cohesionless soil, with weight, indented by a smooth, rigid punch is discussed. The governing equations are hyperbolic, (over)

UNCLASSIFIED

and computational procedures based on the method of characteristics are developed. Detailed numerical solutions obtained on the IBM 7090 computer at The University of Michigan are presented for angles of friction of 20°, 25°, 30°, 35°, and 40°.

UNCLASSIFIED

AD Accession No. UNCLASSIFIED

The University of Michigan, Office of Research Administration, Ann Arbor, Mich. Axially Symmetric Indentation of Cohesionless Soils, by L. A. Larkin. Report No. 04403-10-T, Sept. 1963, 23 p. incl. illus., Project 04403 (Contract No. DA-20-018-ORD-23276)

UNCLASSIFIED

The stress distribution in a cohesionless soil, with weight, indented by a smooth, rigid punch is discussed. The governing equations are hyperbolic, (over)

UNCLASSIFIED

and computational procedures based on the method of characteristics are developed. Detailed numerical solutions obtained on the IBM 7090 computer at The University of Michigan are presented for angles of friction of 20°, 25°, 30°, 35°, and 40°.

UNCLASSIFIED

AD Accession No. UNCLASSIFIED

The University of Michigan, Office of Research Administration, Ann Arbor, Mich. Axially Symmetric Indentation of Cohesionless Soils, by L. A. Larkin. Report No. 04403-10-T, Sept. 1963, 23 p. incl. illus., Project 04403 (Contract No. DA-20-018-ORD-23276)

UNCLASSIFIED

The stress distribution in a cohesionless soil, with weight, indented by a smooth, rigid punch is discussed. The governing equations are hyperbolic, (over)

UNCLASSIFIED

and computational procedures based on the method of characteristics are developed. Detailed numerical solutions obtained on the IBM 7090 computer at The University of Michigan are presented for angles of friction of 20°, 25°, 30°, 35°, and 40°.

UNCLASSIFIED

AD Accession No. UNCLASSIFIED

The University of Michigan, Office of Research Administration, Ann Arbor, Mich. Axially Symmetric Indentation of Cohesionless Soils, by L. A. Larkin. Report No. 04403-10-T, Sept. 1963, 23 p. incl. illus., Project 04403 (Contract No. DA-20-018-ORD-23276)

UNCLASSIFIED

The stress distribution in a cohesionless soil, with weight, indented by a smooth, rigid punch is discussed. The governing equations are hyperbolic, (over)

UNCLASSIFIED

UNCLASSIFIED

and computational procedures based on the method of characteristics are developed. Detailed numerical solutions obtained on the IBM 7090 computer at The University of Michigan are presented for angles of friction of 20°, 25°, 30°, 35°, and 40°.

UNCLASSIFIED

AD Accession No. UNCLASSIFIED

The University of Michigan, Office of Research Administration, Ann Arbor, Mich. Axially Symmetric Indentation of Cohesionless Soils, by L. A. Larkin. Report No. 04403-10-T, Sept. 1963, 23 p. incl. illus., Project 04403 (Contract No. DA-20-018-ORD-23276)

UNCLASSIFIED

The stress distribution in a cohesionless soil, with weight, indented by a smooth, rigid punch is discussed. The governing equations are hyperbolic, (over)

UNCLASSIFIED

UNCLASSIFIED

and computational procedures based on the method of characteristics are developed. Detailed numerical solutions obtained on the IBM 7090 computer at The University of Michigan are presented for angles of friction of 20°, 25°, 30°, 35°, and 40°.

UNCLASSIFIED